arXiv:2606.31845v1 [cs.CL] 30 Jun 2026

Explicit Fuzzy Logic in the Feed-Forward Layer

Self-Forgetting Quantifiers Discover Legible Grammatical-Licensing Detectors

Mark Oskin
Professor
School of Computer Science and Engineering
University of Washington
mhoskin@uw.edu

June 2026

Abstract

The feed-forward (FFN) sublayer is where a transformer materializes the conjunctions and distinctions its attention has gathered—yet its standard form, a pointwise activation of a linear projection, exposes no account of *what* it computes. We study a parameter-neutral replacement in which each hidden unit is an explicit fuzzy set operation on sigmoid-bounded $[0, 1]$ membership values: intersection $A \cdot B$ and set-difference $A \cdot (1 - B)$, the latter a bounded, *positive* encoding of negation ("A but not B") that a gated or bilinear unit structurally lacks. We call this a negation-capable FFN (NC-FFN). On a controlled reasoning probe (N-bit parity in pure feed-forward stacks), bounded multiplicative units are the most parameter-efficient reasoning basis at shallow depth; at language-model scale (125M parameters, OpenWebText), NC-FFN ties the GELU baseline's perplexity at equal parameters, with every unit carrying explicit logical form. But two limits emerge from the same cause. Genuine two-operand logic localizes sharply to the embedding-adjacent layer and *erodes* toward soft gating under language-model training; and the model's one robust grammatical deficit is concentrated in *licensing* and *quantifiers*—precisely the sequence-level constructions that within-token set operators cannot express. Our central result resolves both at once. We add a small, parameter-neutral block of fuzzy *quantifiers* over the sequence—a soft existential and a soft proportion, each with a per-unit *learned forgetting rate* initialized at the non-forgetting (sticky) limit. This recovers the grammatical deficit at epoch one—halving the wider gap that opens by epoch two—and modestly leads the baseline on LAMBADA, while making the FFN markedly more legible. The logical structure now *holds and migrates into depth* rather than eroding; the learned decay *un-learns its own stickiness*—every unit forgets within a few tokens (median half-life $\sim$1.5; *zero* near-permanent units)—so the quantifier is a local, predictive operator, not a latch; and at the semantic layers the units read, without dictionary learning, as grammatical *licensing detectors*. Each fires on a grammatical *licensor* (a comparative, a passive participle, a negative-polarity item) and its $\sim$1.5-token memory carries the membership forward to predict the licensed function word (*than*, *by*, *nor*)—the decay having tuned itself to the grammatical-licensing window. This legibility is localized (a few percent of the network, concentrated at the late layers) and free only up to a partition: a *fully* Boolean FFN with no stabilizing GELU fraction still diverges in training, leaving an end-to-end-legible model an open optimization problem. But within those bounds the result is a parameter-neutral, language-model-quality transformer that contains a readable, interpretable-by-construction grammatical mechanism—an explicit account not just of *what* a feed-forward layer represents but of *how* it licenses.

1 Introduction

Mechanistic interpretability has made the most progress where computation is structurally exposed: attention patterns are legible because attention is, by construction, a weighted routing of values, and induction or copy circuits can be read off the QK/OV structure. The feed-forward sublayer, which holds the majority of a transformer's parameters and is widely argued to be where factual and feature-level computation lives (Geva et al., 2021), is far less transparent: a pointwise activation of a linear projection is a dense, polysemantic, sign-agnostic object whose *operation* on its inputs has no native reading. Post-hoc dictionary methods

recover *what* directions a layer represents (Bricken et al., 2023; Cunningham et al., 2024), but not *how* the layer combines them.

We take a complementary, architectural route: choose an FFN whose *combination rule is explicit*, and ask what that costs and reveals. The FFN is a natural home for set logic—it is where attention's gathered features are conjoined into "this token is a verb *and* the subject is plural" or "a quotation *but not* a heading." The last example is the crux. Negation is cheap to *state* but awkward to *represent*: a raw feature direction has no notion of "absence," so "not B" has no clean positive form. The fix, known from logical-query embeddings over knowledge graphs (Ren and Leskovec, 2020), is to make features *bounded* memberships in $[0, 1]$, a space closed under complement, so that "not B" is simply $1 - B$. Embedding the set operators of fuzzy logic— intersection $A \cdot B$, set-difference $A \cdot (1 - B)$, with the complement supplying negation—into the transformer FFN gives a layer in which every hidden unit is a named AND/AND-NOT of two operands, at no change to the parameter budget, head configuration, or attention. We call it a negation-capable FFN (NC-FFN); "capable" is an architectural property, not a performance promise.

The operators, the multiplicative-FFN form (GLU and bilinear variants), the operator-softening optimization pathology, and the negation-via-complement idea are each established prior art (Section 2); our contribution is their assembly inside a transformer language model and an empirical account of what it does. The account has five parts: four that characterize NC-FFN itself, and a fifth that extends it with a sequence-level operator and yields the paper's headline result.

Capability (Section 5). The motivating question—does a more *structured* component reason more *compactly*?—is not answerable from perplexity, which rewards distributional fit, not reasoning. We isolate it with a controlled probe: N-bit parity, the canonical function that is easy for products and hard for sums, learned by pure feed-forward stacks of each FFN type. Measuring the largest N each solves as a function of width and depth turns "reasoning capacity" into a number. The result is a clean dissociation: *bounded* multiplicative units (NC-FFN, sigmoid-bilinear) are the most parameter-efficient reasoning basis at shallow depth—a single layer outreaches strictly larger GELU—while *unbounded* bilinear products are useless shallow but compose through depth. The two properties our architecture toggles, multiplicativity and bounding, turn out to control two different axes of reasoning efficiency. The small networks here are a controlled instrument for measuring capability, not a scale claim.

Language modeling (Section 6). As a 125M-parameter language model, NC-FFN is a faithful parameter-neutral drop-in: it ties the GELU baseline on perplexity (and the tie tightens with training), with a small, persistent deficit on grammatical structure (BLiMP). We attribute the deficit not to a missing capability but to capacity *allocation*: a bounded multiplicative unit exposes fewer independent standalone features per parameter than an unbounded activation, and ordinary language wants standalone features. The capability the architecture buys is real but *dormant* for next-token prediction, which does not call for it.

Legibility and its dynamics (Section 7). Every NC-FFN unit carries explicit logical form, and a small subset reads as recognizable predicates with no dictionary learning. Genuine two-operand logic localizes sharply to the embedding-adjacent layer; the features the readable units track are *causally used* even though the units are individually redundant. Most strikingly, the network's logical content is *dynamic and task-shaped*: trained on a task that rewards multiplicative reasoning, the Boolean structure *crystallizes* precisely at the grokking transition; trained as a language model, which does not reward it, the same structure *erodes* toward soft gating. The architecture keeps the logic the task pays for.

A trainability boundary (Section 8). The stabilizing GELU majority beside the Boolean block is not optional. As the Boolean fraction rises the model trains longer but then diverges sooner, and a *fully* Boolean FFN diverges within the first ∼16k steps; the obvious remedies—bounding the residual write, a parallel linear highway—only delay it, implicating a saturated-product gradient pathology rather than the write magnitude. Legibility is thus free only up to a partition, and an end-to-end-legible model is gated on removing this instability.

Self-forgetting quantifiers and legible licensing (Section 9). Two of the findings above are limitations with a shared cause: the two-operand logic erodes and localizes to layer 0, and the grammatical deficit concentrates in *licensing* and *quantifiers*— constructions about whether a feature occurred *earlier in the sequence*, which NC-FFN's within-token operators cannot express. We add the missing primitive: a parameter-neutral block of fuzzy quantifiers over the sequence (a soft existential and a soft proportion) with a per-unit *learned forgetting* rate, initialized at the non-forgetting (sticky) limit. It resolves both limitations at once. It recovers the grammatical deficit at epoch one—halving the wider epoch-two gap—and leads the baseline on LAMBADA; the logical structure now *holds and migrates into depth* instead of eroding; the learned decay *un-learns* its sticky initialization—every unit forgets within a few tokens—so the quantifier is a local, predictive operator rather than a latch; and at the semantic layers the units read, without dictionary learning, as grammatical *licensing detectors*, each firing on a grammatical licensor and carrying it forward—on a ∼1.5-token memory that the decay has tuned to the licensing window—to predict the licensed function word. The legibility is localized, not network-wide, but it is a readable, interpretable-by-construction grammatical mechanism at no parameter or language-model-quality cost.

Together these say that an explicit-combination FFN is a viable, parameter-neutral component that reasons more compactly on tasks that need it and exposes *how* it computes—at a modest, well-localized cost; that "how much logic" is not a fixed property of the architecture but a readout of what its training objective rewards; and that giving the feed-forward layer an explicit *sequence* operator, free to learn how long to remember, turns NC-FFN's hardest grammatical failures into its most legible mechanism—a bank of self-forgetting quantifiers that compute readable grammatical licensing.

2 Related Work

NC-FFN sits at the intersection of several mature lines of work: gated and multiplicative feed-forward layers, differentiable fuzzy logic, set-operator embeddings for logical query answering, and the interpretability of transformer feed-forward (FFN) sublayers. The individual ingredients are all established. Our contribution is one of *placement and lens*: assembling sigmoid-bounded fuzzy set operators—including an explicit complement/negation term—into a parameter-neutral FFN sublayer of a decoder-only language model, and characterizing what that choice does. We organize the prior art accordingly and state, for each line, the precise gap that remains.

2.1 Gated and multiplicative feed-forward layers

Gated Linear Units (GLUs) replace a feed-forward activation with the component-wise product of two linear projections, one passed through a gate (Dauphin et al., 2017). Shazeer (2020) systematized GLU variants for the transformer FFN—GEGLU, SwiGLU, and a purely *bilinear* variant $(xW) \odot (xV)$ with no element-wise nonlinearity—and showed they improve language-model quality at matched parameter count. These are the closest architectural relatives of NC-FFN: a GLU is itself a sigmoid-gated multiplicative unit. The distinction is structural. A GLU fuses a gate and a value into a *single* multiplicatively-gated pathway, whereas NC-FFN places a standard activation block *beside* a separate block of explicit set operations and reads them out through a shared projection; and crucially, no GLU variant carries a complement/negation $(1 - B)$ term or a set-theoretic reading of its products.

Pearce et al. (2025) and Pearce et al. (2024) study the bilinear FFN $g(x) = (W_1 x) \odot (W_2 x)$ in transformer language models specifically as a substrate for *weight-based* mechanistic interpretability: because the layer is a pure bilinear form with no nonlinearity, each output is a quadratic form whose interaction structure can be recovered by eigendecomposition. They report that bilinear MLPs are a competitive, parameter-neutral drop-in for activation MLPs. This is the single nearest piece of prior art to ours, and we treat it as both the behavioral control and the head-to-head interpretability comparison (Sections 4, 7). The differences are specific and load-bearing: bilinear operands are unbounded and signed rather than sigmoid-bounded to $[0, 1]$; there is no complement/negation term; and there is no set-operator semantics. As we show, these are not cosmetic: the sigmoid bounding gives NC-FFN a graceful single-operand fallback that a raw bilinear unit structurally lacks.

Neural Arithmetic Logic Units (Trask et al., 2018) use a sigmoid gate to select between additive and multiplicative pathways for systematic numerical extrapolation—adjacent gated-multiplicative machinery,

but aimed at arithmetic rather than set logic and not used as a general FFN.

2.2 Differentiable fuzzy logic and logic-gate networks

The operators NC-FFN uses are textbook continuous (fuzzy) relaxations of Boolean connectives. The product t-norm realizes conjunction as $A \cdot B$, the strong complement realizes negation as $1 - A$, and set-difference follows as $A \cdot (1 - B)$. Neuro-symbolic frameworks such as Logic Tensor Networks (Badreddine et al., 2022) and Logical Neural Networks (Riegel et al., 2020) build differentiable logical formulae from such operators, and van Krieken et al. (2022) analyze their optimization behavior, showing that gradient descent tends to *soften* crisp fuzzy operators because product-form gates suffer vanishing gradients as operands saturate. Differentiable logic-gate networks (Petersen et al., 2022, 2024) learn, per neuron, one of the sixteen two-input Boolean functions via temperature-annealed relaxations, and achieve strong efficiency on vision benchmarks. These works establish the operators and their optimization pathologies, but always as a *standalone* logical network (typically for vision or tabular data), never as an FFN sublayer inside a transformer trained for language modeling. van Krieken et al. (2022) in particular predicts—in non-transformer settings—the softening we observe; our depth-resolved measurements (Section 7) make this concrete inside a language model and localize where the softening does *not* happen. Pushed past a roughly even split toward a fully Boolean layer, this same saturation pathology no longer merely *softens* the operators but destabilizes training outright (Section 8).

2.3 Quantifiers, aggregation, and learned forgetting

The within-token set operators above have a natural sequence extension—*quantifiers*—and our self-forgetting quantifier block (Section 9) draws on three established lines. First, *quantifier aggregation* in differentiable logic: fuzzy and neuro-symbolic frameworks realize the existential as a maximum (or a soft p-mean/log-sum-exp) and the universal as a mean or product over a domain. Logic Tensor Networks (Badreddine et al., 2022) and Logical Neural Networks (Riegel et al., 2020) build exactly these quantifier aggregations, and van Krieken et al. (2022) analyze their gradients. Our existential (a leaky cumulative maximum) and proportion (a running mean) are the causal, left-to-right specializations of those aggregations over the prefix of the sequence. Second, *learned forgetting*: a decayed cumulative max or moving average with a *learned* per-unit rate is, mechanistically, the forget gate of gated recurrent networks (Gers et al., 2000)—a leaky integrator whose time constant is trained rather than fixed. Our contribution is to give a fuzzy *quantifier* this learned temporal scope, so the operator can learn its own window and, as we find, *un-learn* a sticky cumulative initialization toward a short, predictive memory; to our knowledge prior fuzzy quantifiers aggregate over a fixed or unbounded domain without a learned decay, and none has been placed as an FFN sublayer of a language model. Third, *grammatical licensing*: the constructions our units detect—NPI licensing, comparatives, passives—are the long-distance dependencies that targeted grammatical evaluations such as BLiMP (Warstadt et al., 2020) probe, and that are inherently about whether a licensor occurred earlier in the string. Where the interpretability of licensing is otherwise a post-hoc reading of an opaque model, our quantifier units realize a licensing detector *by construction*.

2.4 Set operators and negation in embedding space

A parallel line uses fuzzy/box/cone set operators to answer logical queries over knowledge graphs. BetaE (Ren and Leskovec, 2020) represents entities as Beta distributions and implements conjunction, disjunction, and—notably—*negation* as a closed operation, motivated by queries of the form "X and Y but not Z." Query2box (Ren et al., 2020), ConE (Zhang et al., 2021), and FuzzQE (Chen et al., 2022) develop related set-operator embeddings, the last using explicit fuzzy logic. These works are the origin of the complement-for-negation idea we adopt, and their motivating use case is essentially identical to ours at the conceptual level. The gap is again placement: the operators live in a dedicated *query-answering head* over a knowledge graph, not as a general-purpose FFN in a language model trained on next-token prediction. An adversarial citation-forward sweep from this literature did not surface any migration of the operators into an LM FFN.

2.5 Interpretability of feed-forward sublayers

A substantial body of work treats the FFN as the locus of interpretable computation: Geva et al. (2021) cast FFN layers as key-value memories, Softmax Linear Units (Elhage et al., 2022a) modify the activation to encourage more interpretable, less polysemantic units, and Codebook Features (Tamkin et al., 2023) bind hidden states to a small set of discrete, nameable codes via a vector-quantization bottleneck—the *interpretable-by-construction* intervention closest in spirit to ours, though it constrains the activation's discreteness rather than, as NC-FFN does, the layer's combination rule. More broadly, individual neurons are known to be *polysemantic* due to superposition (Elhage et al., 2022b), which has motivated dictionary-learning methods—sparse autoencoders— that recover more monosemantic features post hoc (Bricken et al., 2023; Cunningham et al., 2024). NC-FFN relates to this line in two ways. First, like Pearce et al. (2025), it is an architecture chosen partly for interpretability; but where bilinear interpretability is a global, weight-based spectral decomposition, NC-FFN exposes *explicit logical form*—each unit is an AND/AND-NOT of two operands, including a negation a bilinear eigenvector cannot express. Second, our findings are consistent with superposition: the *operands* of NC-FFN units are themselves distributed/polysemantic directions, so the architecture supplies the combination rule for free but not, in general, monosemantic predicates—a small directly-readable subset notwithstanding (Section 7).

2.6 Neuro-fuzzy and fuzzy-membership transformers

Finally, an applied literature combines fuzzy logic with transformers, largely in forecasting, fault diagnosis, and control. The nearest work to ours on keywords is Huang and Raza (2025), which augments a transformer language model with a parallel fuzzy-*membership* feature channel (interpretable per-token features such as part-of-speech cues, sentiment polarity, and boundary flags) graded by differentiable membership functions and fused via a gated adapter with an auxiliary reconstruction loss. This shares the words "fuzzy," "membership," and "language model," but the mechanism is a *side-channel adapter* that injects hand-specified features, not a set-operator FFN computed from the residual stream. It does not implement set operators, has no complement/negation term, and does not replace the FFN.

2.7 Summary

Taken together, the operators (fuzzy t-norms with complement), the multiplicative-FFN form (GLU, bilinear), the optimization pathology (operator softening), and the negation-via-complement motivation (KG query embeddings) are all prior art that we build on. What is, to our knowledge, novel is the specific assembly: *sigmoid-bounded fuzzy set operators, including an explicit complement/negation term, as a parameter-neutral feed-forward sublayer of a decoder-only language model*—and, as the paper's headline extension, a *self-forgetting fuzzy quantifier* over the sequence (a causal existential/proportion with a per-unit learned forgetting rate) as a sublayer of the same model, which we find computes legible grammatical licensing. The defensible fingerprint that distinguishes NC-FFN from its nearest neighbors is the explicit $(1 - B)$ complement inside a transformer FFN: bilinear MLPs have the multiplicative structure but no bounding and no complement (Shazeer, 2020; Pearce et al., 2025); GLUs have the sigmoid gate but no set-operator framing (Shazeer, 2020); differentiable logic networks have the operators but are not transformer LMs (Petersen et al., 2024); the KG-query embeddings have the operators and negation but in a query head (Ren and Leskovec, 2020); and the nearest fuzzy-membership LM (Huang and Raza, 2025) is a side-channel adapter rather than an FFN operator. Our aim is therefore not a new operator but a new view of an old one inside the transformer FFN, and an empirical account of what that view reveals.

3 The NC-FFN Layer

3.1 Background: the transformer FFN

A standard transformer feed-forward sublayer maps $x \in \mathbb{R}^d$ through an up-projection, an element-wise activation, and a down-projection:

$$\mathrm{FFN}(x) = W_o\ \mathrm{GELU}(W_{\mathrm{in}}\, x), \qquad W_{\mathrm{in}} \in \mathbb{R}^{d_{ff} \times d},\ \ W_o \in \mathbb{R}^{d \times d_{ff}}, \tag{1}$$

with $2\,d\,d_{ff}$ parameters. NC-FFN replaces the activation with explicit fuzzy set operations while preserving this parameter budget exactly.

3.2 Fuzzy set operators as hidden units

We read each hidden unit as a fuzzy set-membership value in $[0, 1]$. From the layer input we form two membership vectors via independent linear projections and a logistic nonlinearity,

$$A = \sigma(W_a\, x), \qquad B = \sigma(W_b\, x), \qquad W_a, W_b \in \mathbb{R}^{m\times d}, \tag{2}$$

and combine them with product-form fuzzy operators. The default configuration uses intersection and set-difference,

$$h_\cap = A \odot B \quad (\text{“}A \text{ and } B\text{”}), \qquad h_\setminus = A \odot (1 - B) \quad (\text{“}A \text{ and not } B\text{”}), \tag{3}$$

where $\odot$ is the element-wise product. The complement $1-B$ supplies an explicit, bounded, *positive* encoding of negation: a unit can fire for the presence of one feature and the *absence* of another. This explicit negation primitive is the architectural feature that distinguishes the layer from its multiplicative neighbors—a bilinear or gated unit has no clean *positive* encoding of “A and not B”—and we accordingly call it a *negation-capable* FFN (NC-FFN). We stress that “capable” denotes an *architectural* property, not a performance claim. A standard FFN can *approximate* negated functions; what NC-FFN adds is an explicit, bounded, interpretable negation primitive. And as Section 7 shows, possessing the primitive does not by itself improve—indeed it slightly degrades—performance on negation-sensitive grammar: the name denotes the capability, not its benefit. The combined hidden vector is read out through a single down-projection,

$$\text{NC-FFN}(x) = W_o\, h, \qquad h = [\, h_\cap \,;\, h_\setminus \,] \in \mathbb{R}^{2m}, \qquad W_o \in \mathbb{R}^{d\times 2m}. \tag{4}$$

We refer to a paired (A_i, B_i) and the operations built from it as a *unit*, and to the explicit AND/AND-NOT structure as the unit’s logical *form*.

3.3 Parameter neutrality

For k operators built from a single (A, B) pair, the input side comprises W_a, W_b ($2m$ rows) and the output side W_o has $H = km$ columns, giving $(2m + km)\, d = (2 + k)\, m\, d$ parameters. A pure NC-FFN layer with k operators is therefore parameter-matched to a GELU FFN when

$$(2 + k)\, m = 2\, d_{ff}. \tag{5}$$

Thus NC-FFN does not change the layer’s parameter count, head configuration, or attention; it spends the same budget on constrained multiplicative set operations rather than free, unbounded activations. Because the bounded operators occupy capacity a GELU block would otherwise have, the *effective* flexibility per unit is lower; whether this trades favorably is an empirical question (Section 7).

3.4 The hybrid partition

A pure NC-FFN layer is difficult to train. As operands saturate, the product-form gradients vanish (the pathology analyzed by van Krieken et al. (2022)), and an all-positive, bounded basis is a poor substrate for the output projection; in our experiments a pure layer trains normally for thousands of steps and then diverges abruptly, a conditional instability we characterize in Section 8. We therefore use a *hybrid partition*: a fraction of the layer budget is given to a standard GELU “gradient highway” and the remainder to the set-operator block, read out through one shared W_o:

$$h = [\, \text{GELU}(W_g\, x) \,;\, h_\cap \,;\, h_\setminus \,], \qquad W_g \in \mathbb{R}^{g\times d}. \tag{6}$$

With g GELU units and m operator pairs, the input side is $(g + 2m)d$ and the output side $Hd = (g + km)d$, so parameter neutrality with a d_{ff} GELU FFN holds when

$$m = \frac{2\, d_{ff} - 2g}{2 + k}. \tag{7}$$

We parameterize the split by the GELU budget fraction $\rho = g/d_{ff}$; our main model uses $\rho = 0.75$ (a GELU-dominant 3:1 split). Two further details make the partition fair. The Boolean output columns of W_o are *zero-initialized* (re-zeroed after standard initialization), so the layer begins as a pure g-wide GELU FFN and the set-operator block is wired in only if training finds it useful (a function-preserving initialization). And because the bounded Boolean block has a capped output norm while GELU is unbounded, we apply a per-block RMS normalization (a single scalar gain per block, parameter-negligible) before W_o so the two blocks enter the read-out on weight-decay-fair footing.

3.5 A property: graceful degeneration

The sigmoid bounding endows NC-FFN with a property its bilinear cousin lacks. If the second operand of a unit becomes uninformative—$W_b \to 0$, hence $B = \sigma(W_b x) \to \frac{1}{2}$, a *non-zero* constant—then $h_\cap, h_\setminus \to \frac{1}{2}A$, and the unit collapses to a single-operand, sigmoid-gated feature: an ordinary bounded activation. The Boolean unit can therefore *relax* into a normal activation MLP wherever two-operand logic is not useful. A raw bilinear unit $(W_1 x)(W_2 x)$ has no such fallback: a linear projection has no non-zero constant state, so zeroing one operand kills the unit, and its only single-operand mode is the unbounded quadratic $(wx)^2$ obtained when $W_1 \parallel W_2$. This difference—a graceful single-operand fallback present under sigmoid bounding and absent for raw bilinear—is central to interpreting the depth-resolved behavior we report in Section 7, and motivates the bilinear control of Section 4.

4 Experimental Setup

4.1 Models

Our primary model is a 12-layer, GPT-2-small-scale decoder ($d = 768$, 12 heads, $d_{ff} = 3072$, sequence length 2048, 125.1M parameters). The NC-FFN model replaces every FFN with the hybrid layer of Section 3.4 at $\rho = 0.75$ and operators $\{\cap, \setminus\}$ (intersection and set-difference), giving, per layer, $g = 2304$ GELU units and $m = 384$ operator pairs (768 Boolean hidden units). The parameter-matched baseline (GELU) is an identical architecture with standard GELU FFNs. We additionally use a 4-layer variant of each architecture for cheaper ablations.

4.2 Training

All models are trained on OpenWebText with the same recipe: batch size 16, sequence length 2048, AdamW ($\beta = (0.9, 0.95)$, weight decay 0.1), peak learning rate 3×10^{-4} with 2000 warmup steps and cosine decay to 10% of peak over one epoch (272,687 steps). We checkpoint weights at 50k-step intervals (50k–250k) in addition to epoch boundaries, which enables the training-trajectory analyses in Section 7. A second epoch (analyzed in later sections) continues from the epoch-1 optimizer state with a fresh cyclical-cosine cycle (warmup 500, same peak and decay), matching the multi-epoch schedule of the baseline.

4.3 Evaluation

We report dev perplexity and zero-shot accuracy on a standard small-model suite via the LM-EVAL harness (Gao et al., 2021): LAMBADA (Paperno et al., 2016), BLiMP (67 subtasks) (Warstadt et al., 2020), ARC-Easy (Clark et al., 2018), HellaSwag (Zellers et al., 2019), and WinoGrande (Sakaguchi et al., 2020). At this scale ARC-Easy, HellaSwag, and WinoGrande carry little discriminating signal for all models—HellaSwag and WinoGrande sit at or near the random baseline—so we treat LAMBADA (long-range semantic prediction) and BLiMP (grammatical structure, with per-subtask resolution) as the discriminating benchmarks and report the rest for completeness. All evaluations use a right-padded batching adapter; we verified the adapter against published GPT-2 LAMBADA accuracy.

4.4 Probing the Boolean block

We use three complementary, inference-only probes, all run on CPU from saved checkpoints.

Engagement and realization. For each layer we capture the FFN input on held-out tokens and recompute the operand activations A, B and the two block contributions to the residual write through the shared W_o. We report (i) the *bool share*—the fraction of the per-token FFN write carried by the Boolean block—as a measure of how much the model *uses* the operators, and (ii) operand statistics ($\bar{A}$, $\bar{B}$, and $\overline{A \cdot B}$) as a measure of whether genuine *two-operand* logic is *realized*: a unit doing real set logic must have both an informative A and an informative B, whereas a unit with $B \approx 0.5$ has degenerated to single-operand gating (Section 3.5).

Causal ablation. To measure necessity rather than mere activation, we zero the Boolean output columns of W_o (globally, or one layer at a time) and measure the perplexity penalty on a fixed, paired held-out batch. Because a large ablation grows more damaging over training simply through co-adaptation, we include a *control*: ablating an equal-sized random subset of the GELU columns, which isolates whether a growing Boolean ablation penalty is Boolean-specific or generic.

Logic-unit scout. To find units doing genuine two-operand logic and read their predicates, we rank unit pairs by two criteria: A is a *selective* sparse gate (low firing rate) and B is *informative when A fires* (it takes both high and low values on A-firing tokens, rather than a constant). For the resulting units we read the predicate by collecting the tokens that trigger the A-gate and then, among A-firing positions, the tokens that B *includes* ($A \cdot B$) versus *excludes* ($A \cdot (1 - B)$)—rendering the unit's AND/AND-NOT statement directly.

4.5 The bilinear control ladder

Because our central claim is about the *view*—fuzzy set operators as an FFN—rather than a new operator, the key control is whether NC-FFN behaves and explains differently from a matched bilinear FFN, the nearest prior art (Pearce et al., 2025). A bilinear *layer* is itself competitive with GELU (Shazeer, 2020; Pearce et al., 2025), so it is a fair baseline rather than a weakened one, and a measured difference is attributable to what we change. We therefore compare a ladder of parameter-neutral $\rho = 0.75$ hybrids that differ *only* in the non-GELU block: (i) NC-FFN $[A \cdot B,\ A \cdot (1 - B)]$ (bounding + complement); (ii) a *sigmoid-bilinear* block $\sigma(W_1 x) \cdot \sigma(W_2 x)$ (bounding, no complement), which—unlike raw bilinear—shares NC-FFN's graceful degeneration and so isolates the contribution of the complement/set-operator structure; (iii) a *raw bilinear* block $(W_1 x) \cdot (W_2 x)$ (neither), which isolates the contribution of sigmoid bounding; and (iv) the GELU anchor. We realize this ladder in pure form as the four FFN types of the capability probe (Section 5), and the same parameter-neutral partition can be instantiated at language-model scale as a control.

5 Results I: Reasoning Capability

Perplexity cannot answer our motivating question—whether a more structured FFN reasons more compactly—because next-token prediction rewards distributional fit, not reasoning, and a model can be fluent without composing anything. We therefore isolate capability with a controlled probe and measure it as a number.

5.1 A capability probe: parity in pure feed-forward stacks

N-bit parity is the canonical separator of additive from multiplicative computation. In the ± 1 encoding it is a single product $\prod_i x_i$, trivial for a multiplicative unit to *represent* but requiring exponentially many threshold units—and offering no benefit from depth—for a purely additive (e.g. ReLU/GELU) one. It is exactly the kind of compositional function a structured component should handle more cheaply, and it is uncontaminated by the distributional statistics that let language models fake competence.

To attribute any difference to the FFN alone we remove attention entirely: each model is a pure feed-forward stack—a linear embedding of the N input bits ($\to \mathbb{R}^{128}$), L residual FFN blocks, and a linear head—trained directly to predict the parity bit. We sweep the FFN *type*, the depth $L \in \{1, 2, 3, 4\}$, the hidden width d_{ff}, and the difficulty $N \in \{1, \ldots, 12\}$, with multiple seeds, and summarize each configuration by its *reach*: the largest N it solves (best accuracy ≥ 0.75, averaged over seeds). Four FFN types isolate the two properties our architecture toggles, here in *pure* form (no GELU partition, so the block is entirely the

Table 1: Reasoning reach (largest N-bit parity solved, mean over 5 seeds) versus depth L, pure feed-forward stacks at $d_{ff} = 256$. Bounded multiplicative units (NC-FFN, sigmoid-bilinear) dominate at shallow depth; unbounded raw-bilinear is useless shallow but climbs steeply with depth; GELU plateaus between.

FFN type	$L = 1$	$L = 2$	$L = 3$	$L = 4$
GELU (additive)	6	6	7	7
Raw-bilinear (mult., unbounded)	2	4	7	8
Sigmoid-bilinear (mult., bounded)	7	8	7	7
NC-FFN (mult., bounded, +complement)	**8**	**8**	7	**8**

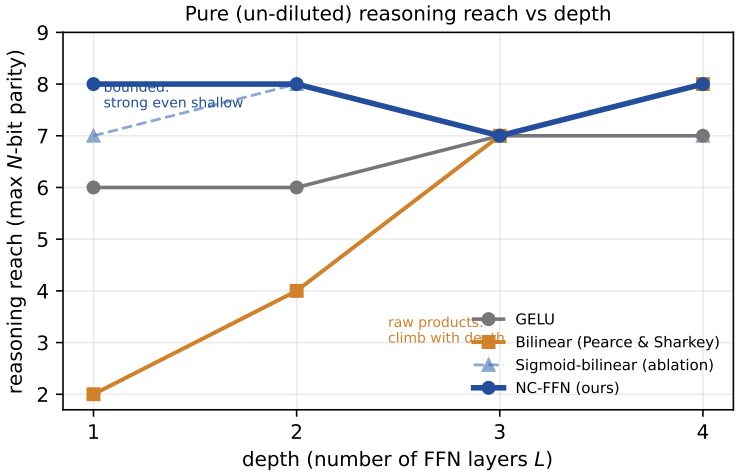

Figure 1: Reasoning reach versus depth for the four pure FFN types. The two *bounded* multiplicative lines (NC-FFN, sigmoid-bilinear) start high and stay high; *unbounded* raw-bilinear climbs steeply from a useless-shallow base, tracking the degree-doubling of composed products; the additive GELU baseline plateaus in between. Bounding buys width-efficient shallow reasoning; unbounding buys depth-composition.

named operator): GELU (additive); *raw-bilinear* $(W_1x)\cdot(W_2x)$ (multiplicative, unbounded); *sigmoid-bilinear* $\sigma(W_1x)\cdot\sigma(W_2x)$ (multiplicative, bounded, no complement); and NC-FFN $[\sigma(W_ax)\sigma(W_bx), \sigma(W_ax)(1-\sigma(W_bx))]$ (multiplicative, bounded, with complement). The networks are deliberately small: they are a measuring instrument for per-parameter reasoning efficiency, not a scale claim.

5.2 Bounding and depth control two different axes of reasoning

Figure 1 and Table 1 report reach as a function of depth at fixed width. The picture is a clean dissociation rather than a single ordering.

Bounding buys width-efficient, shallow reasoning. At a single layer, the bounded multiplicative units are the most parameter-efficient reasoning basis by a wide margin: NC-FFN reaches N=8 and sigmoid-bilinear N=7, against GELU's 6 and raw-bilinear's 2. A degree-2 layer cannot solve parity-8 by algebraic composition; the bounded units do it through *width*—combining sigmoid-bounded product terms in the read-out—and strikingly few suffice. Sweeping the width at fixed L=1 (Table 2), each arm sits at a flat, *width-robust* shallow ceiling that is already reached by d_{ff}=16 and unchanged out to 256: NC-FFN 8, sigmoid-bilinear 7, GELU 6, and raw-bilinear below 5 at every width. This is exactly where bounding matters: products of $[0, 1]$ values remain in $[0, 1]$, so the read-out can stably combine them, whereas an unbounded raw product explodes under summation—which is why raw-bilinear is useless at one layer *at any width*. Bounding is thus not a legibility nicety; it is what makes a multiplicative unit a usable shallow reasoning basis.

Table 2: Reach versus hidden width at fixed depth L=1 (mean over 4 seeds). The shallow ordering is width-robust—each arm sits at a flat ceiling from d_{ff}=16 to 256. Raw-bilinear does not reach N=5 at any width (it solves only $N \leq 2$).

FFN type	d_{ff}=16	32	64	128	256
GELU	6	6	6	7	6
Raw-bilinear	< 5	< 5	< 5	< 5	< 5
Sigmoid-bilinear	7	7	7	7	7
NC-FFN	**8**	**8**	**8**	**8**	**8**

Unbounding buys depth-composition. Raw-bilinear shows the opposite profile: its reach climbs $2 \to 4 \to 7 \to 8$ with depth, tracking the algebraic fact that composing products doubles their degree per layer (2^L). Unbounded products cannot be summed in width but *can* be multiplied in depth, so depth is their only route to parity—and a clean one. The bounded units do not gain comparably from depth (they are already near ceiling at L=1, and the sigmoid squashes degree growth across layers), so the two strategies are genuinely complementary: bounding trades depth-composition for width-stability.

The additive baseline plateaus. GELU sits between the two at every depth (6–7), neither width-efficient nor depth-composing for parity—consistent with parity being additive-hard at any depth. Its near-flatness across L confirms that, unlike the multiplicative units, it derives no compositional benefit from added layers here.

5.3 The complement adds a shallow margin

The two bounded arms differ only in the explicit complement, and NC-FFN edges sigmoid-bilinear where depth cannot be leaned on: at L=1, reach 8 versus 7. With the operand budget tightest—one layer—getting both $A{\cdot}B$ and $A{\cdot}(1-B)$ from a single shared operand pair, rather than spending a separate pair to recover the complement by sign-flip, is worth a parity bit. The margin is modest and concentrated at shallow depth; we do not claim the complement adds reasoning power beyond the bounded multiplicative basis it shares with sigmoid-bilinear—its larger contribution is to legibility (Section 7). The honest summary is that *multiplicativity* and *bounding* are the load-bearing capability properties, and the explicit negation is a small efficiency-and-legibility addition on top.

Scope. These are controlled measurements on a single synthetic family with a fixed optimization budget; the absolute reach values depend on width, steps, and seeds, and a longer budget would likely let raw-bilinear's degree-2^L advantage carry it higher at L=4. What is robust, and what we rely on, is the *qualitative dissociation*—bounded-shallow versus unbounded-deep, with the additive baseline between—which holds across the sweep.

6 Results II: Language Modeling

We now place NC-FFN in its target setting—a 125M-parameter decoder trained on OpenWebText—and ask the necessary viability question: is an explicit-combination FFN a faithful parameter-neutral drop-in, and what does the constraint cost? The answer is a clean tie on perplexity with a small, well-localized cost on grammar, and—importantly—no language-model *benefit*, exactly as the capability result predicts.

6.1 A perplexity tie that tightens, and no semantic gain

At equal parameters, NC-FFN matches the GELU baseline on perplexity, and the match tightens with training (Table 3): the dev-perplexity gap falls from +0.11 after one epoch to +0.04 after two, as the deep Boolean blocks relax toward GELU-equivalent capacity (Section 7). On the discriminating downstream benchmarks the model is at parity or slightly behind. A single-seed epoch-1 LAMBADA edge (accuracy

Table 3: Language-model evaluation, 12L, parameter-matched, across two epochs. The perplexity tie *tightens* with training; LAMBADA is a tie (the epoch-1 edge washes out); the BLiMP deficit *persists and widens*.

	Epoch 1		Epoch 2	
Metric	GELU	NC-FFN	GELU	NC-FFN
Dev perplexity ↓	19.00	19.11	18.32	18.36
LAMBADA acc. ↑	0.254	0.262	0.275	0.273
LAMBADA ppl. ↓	109.4	102.4	78.1	85.5
BLiMP (67) ↑	0.807	0.788	0.823	0.790

+0.009, perplexity −7) does *not* survive a second epoch—by epoch two the baseline is marginally ahead on both—so we read LAMBADA as a tie and make no semantic-advantage claim. The floor benchmarks (HellaSwag, WinoGrande) are at chance for both models at this scale.

6.2 A small, persistent grammatical deficit—and where it lives

The one robust downstream signal is a BLiMP deficit, and it *widens* with training rather than closing: the baseline's grammar improves over the second epoch ($0.807 \rightarrow 0.823$) while NC-FFN's stays flat ($0.788 \rightarrow 0.790$), so the gap grows from -0.019 to -0.033 (well outside within-sample error). The deficit is concentrated, not diffuse: across the 67 subtasks the baseline wins 36 to 22 (9 ties), with losses clustered in *island/long-distance extraction* (*left-branch-island* −0.31, *coordinate-structure* −0.25), *NPI licensing* (*npi-present-1* −0.18, *matrix-question-npi* −0.14), and *quantifiers* (−0.10 to −0.13). There is an irony worth stating plainly: NPI licensing—the grammatical reflex of negation and polarity—is among the negation-motivated architecture's *weakest* areas (lone exception: *only-npi-licensor-present*, its largest gain at +0.23). The architectural negation primitive does not translate into better handling of grammatical negation.

6.3 Why: capacity allocation, not missing capability

We attribute the deficit to capacity *allocation* rather than an inability. Per parameter, the hidden units cost the same as GELU's ($2d$ each), but a Boolean unit is a *more constrained* basis. A pair's two outputs satisfy $A{\cdot}B + A{\cdot}(1-B) = A$, so the pair spans only $\{A,\ A{\cdot}B\}$: one standalone sigmoid feature and one product, with the second operand spent entirely inside the product. Two GELU units of the same parameter cost instead give two *independent* standalone features. Ordinary language modeling is hungry for standalone, threshold-like features (which is what grammar needs), and mostly does not need the products—so a quarter of NC-FFN's budget is, for this task, spent on units of lower marginal value. Its effective standalone-feature capacity is accordingly between that of a strictly narrower GELU model and the full baseline, which is the deficit's size and sign. This is the same allocation that the capability probe rewards: the products that cost grammar a little are exactly what reason on parity. The architecture's capability is real but *dormant* for next-token prediction, which does not call for it—so it ties, at a small constant cost, rather than winning or losing decisively.

7 Results III: Legibility and Its Dynamics

Because every NC-FFN unit is a named AND/AND-NOT of two operands, the layer admits questions an opaque activation does not: *where* in the network is genuine two-operand logic realized, *which* units are causal, and *how* does the logical content change over training? We answer these with inference-only probes (Section 4) and close with the result we find most telling—that the amount of logic is not a property of the architecture but of what the task rewards.

Table 4: Boolean-block statistics by layer (final checkpoint). *bool share*: fraction of the FFN residual write carried by the Boolean block (engagement, depth-uniform). $\overline{A \cdot B}$, $\bar{A}$, $\bar{B}$: operand realization—only layer 0 shows informative two-operand structure.

Layer	0	1	2	4	6	8	10	11
bool share	0.42	0.31	0.39	0.47	0.42	0.44	0.47	0.30
$\overline{A \cdot B}$	**0.134**	0.017	0.015	0.040	0.014	0.025	0.013	0.034
$\bar{A}$	**0.286**	0.032	0.028	0.076	0.030	0.051	0.027	0.067
$\bar{B}$	**0.484**	0.504	0.501	0.504	0.506	0.503	0.508	0.506

Table 5: Operand fate over all Boolean units (epoch-one checkpoints), averaged across the 12 layers. *One-operand*: one operand collapsed to ≈constant (the single-operand relaxation of Section 3.5). *Independent*: both operands active, correlation at/below a matched cross-unit floor (distinct, non-duplicated signal). *Redundant*: both active but the second tracks the first above the floor. The split is almost never a redundant copy.

Model	One-operand	Independent	Redundant
+DECAY+GATE	42.9	54.0	**3.2**
+DECAY	43.4	54.8	**1.8**
+QUANT	48.6	50.6	**0.9**

7.1 Engagement is depth-uniform; realization is localized to layer 0

The Boolean block is heavily and uniformly *used*: its share of the per-token FFN residual write is 0.30–0.47 at every layer, with no decay toward the top (Table 4). But genuine *two-operand* realization is sharply localized. Only at layer 0 is the second operand informative ($\bar{B} = 0.48$, away from the uninformative 0.5) with a sizable intersection signal ($\overline{A \cdot B} = 0.13$); at every deeper layer $\bar{B}$ collapses to ≈ 0.50 and $\overline{A \cdot B}$ drops by an order of magnitude, so the units have degenerated to the single-operand gates of Section 3.5. We summarize this as a *recruitment-versus-realization* gap: the partition is recruited everywhere but its set-operator semantics are realized only at the embedding-adjacent layer—a contrarian result, cutting against the intuition that depth sharpens abstraction.

7.2 The split is used or cleanly retired, almost never redundant

A split representation invites a specific failure—the two operands collapsing into a *redundant* copy, so the layer pays for a duplicate. Section 3.5 predicts a different failure mode instead: an unused unit drops *one* operand and reverts to an ordinary single-operand activation. We test this directly, classifying every Boolean unit from the joint statistics of its operands across tokens. An operand is *collapsed* when its activation variance is negligible; a surviving pair is *redundant* when B correlates with A above the 99th percentile of a matched cross-unit floor, and *independent* otherwise. The three fates are exhaustive and consistent across the quantifier ladder (Table 5). *Redundant* duplicate pairs are **under** 5% in every variant, with median operand correlation ≈ 0 (frequently negative—the "A and not B" regime). The remainder divides into units that retire one operand to the single-operand gate of Section 3.5 ($\approx 45\%$) and units whose operands stay both active and independent ($\approx 50\%$). The split therefore does not waste capacity on a duplicate: where two-operand logic is not used, a unit relaxes to a plain activation, exactly the graceful degeneration the bounding affords. We stress that "independent" is a far weaker condition than the *informative* two-operand signal of Table 4 (concentrated at layer 0) or the crisp predicates of Table 7: an operand may vary around its uninformative midpoint, contributing distinct but small-magnitude modulation. The only claim here is the one the architecture promises—that the second operand, when present, is not a redundant copy of the first.

Table 6: Causal ablation: loss penalty (nats) for zeroing Boolean output columns, paired on a fixed 131k-token batch. The GELU-chunk control ablates an equal number of random GELU columns/layer.

Ablation (Δloss, nats)	50k	100k	final
All Boolean blocks	+3.20	+3.74	+5.16
GELU-chunk control	+1.11	+1.62	+4.63
Layer-0 Boolean only	+2.08	+2.13	+2.23
(as perplexity)	+220	+210	+187

Table 7: The logic–fuzzy spectrum at layer 0. Units binned by B-discrimination when A fires (≈ 0 = soft single-operand gating). A deep layer (6) has no logic tail.

B-disc. bin	0–.02	.02–.05	.05–.10	.10–.15	.15–.20	.20–.30	active
Layer 0	221	14	14	5	2	1	257
Layer 6	5	0	0	0	0	0	5

7.3 Causal ablation: layer-0 is irreplaceable, deep blocks are redundant capacity

Activation statistics measure use, not necessity. Zeroing the Boolean output columns and measuring the perplexity penalty on a fixed held-out batch gives the causal picture (Table 6). Removing *only layer 0*'s Boolean block costs ≈ 187 perplexity (+2.23 nats)—the single most load-bearing FFN component in the network, and the one layer doing genuine two-operand logic. Deeper layers are individually near-removable (1–6 ppl each) but *collectively* essential: ablating all Boolean blocks costs +5.16 nats, well above the $\approx$ 3.5 nats of the summed single-layer penalties—a distributed, redundant Boolean pathway across depth. A matched control (an equal-sized random GELU-column ablation) grows nearly as steeply over training (+1.11 $\rightarrow$ +4.63), so most of the all-block growth is generic co-adaptation, not Boolean necessity; what survives the control is that Boolean columns are more load-bearing than GELU columns at every checkpoint, an advantage that narrows by the end—the deep blocks converging toward generic capacity, the localized layer-0 block remaining decisive.

7.4 Readable units, and a logic–fuzzy spectrum

Requiring a selective A-gate and a genuinely two-valued B yields a small set—fewer than ten strict two-operand units in the whole 12-layer model, almost all at layer 0—that read as recognizable predicates *without* dictionary learning. The clearest (layer-0, A-firing rate 0.085) is a function/content discriminator: its A-gate fires for high-frequency function tokens (“`,`”, “`\n`”, “ `the`”, “ `.`”); the $A \cap B$ branch keeps the function tokens and the $A \setminus B$ branch isolates content tokens (“ `Antonio`”, “ `Nintendo`”)—a clean “frequent token AND NOT content word.” Others encode sentence/line-boundary context and a code-syntax-versus-identifier split. But this is a *spectrum*, not a dichotomy (Table 7): of 257 active layer-0 units, 221 have negligible B-discrimination (soft single-operand gating), with a thin tail of crisp logic; a deep layer has no tail at all. The directly-readable units are few and encode low-level structural distinctions; the bulk of operands are distributed and polysemantic, exactly as superposition predicts (Elhage et al., 2022b). The architectural payoff is not universal monosemanticity but that *even the distributed units carry explicit logical form*—each a known AND/AND-NOT —whereas a GELU or bilinear ensemble is distributed *and* opaque in its operation.

7.5 Redundant units, causally-used features

Are the readable units *causal*? Single-unit interventions say no: ablating the function/content unit's readout, or flipping its B operand, changes next-token predictions negligibly ($< 10^{-3}$ nats). This is redundancy, not irrelevance: training distributes each feature across many carriers, so no single unit is necessary (consistent with the super-additive block ablation above). The correct test is at the level of *features*: ablating a feature *direction* removes it from all carriers at once. Projecting the function/content axis out of the layer-0

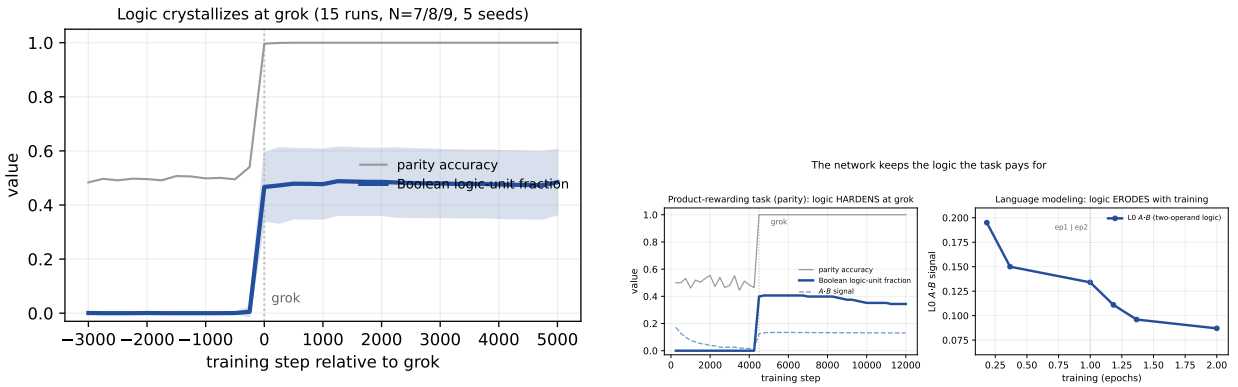

Figure 2: The logical content is task-shaped. **Left:** on a product-rewarding task (parity), the fraction of units doing two-operand logic snaps from ≈ 0 to ≈ 0.48 *at* the grok step (grok-aligned mean over 15 runs, band = s.d.). **Right:** under language-model training, the layer-0 two-operand signal *erodes* monotonically across two epochs. Same Boolean block, same probe, opposite trajectories.

output costs 148× the loss of a random direction of equal norm, localized to function-word positions (1.6×); the sentence-boundary unit's own axis gives 228× a random direction and 4.2× localization. The faithful statement is therefore not "this unit caused token X" but **"a unit's firing is faithful evidence that a causally-used feature is active here"**—and, methodologically, that under a redundant network one must ablate *directions*, not units, or systematically understate importance.

7.6 The logic is task-shaped: it hardens where the task pays, erodes where it does not

The most revealing property is dynamic. The layer-0 two-operand signal does not sharpen with training; it *softens*—$\overline{A \cdot B}$ decays monotonically across both epochs ($0.195 \to 0.150 \to 0.134 \to 0.111 \to 0.096 \to 0.087$), as the products relax toward the single-operand gating that language modeling rewards (Section 6). Crisp two-operand logic is an *early*-training feature that erodes; what persists is the depth-localization, the engagement, and feature-level causality (the sentence-boundary axis is still 442× a random direction at epoch two), not unit-level crispness.

Is the erosion intrinsic, or a readout of the objective? We test the converse directly. Train the *same* Boolean block, with the same probes, on a task that *rewards* products—parity at the solvable edge—and track the logic over training. It does the opposite: the Boolean structure *hardens*, and the hardening coincides exactly with generalization. Across 15 runs ($N \in \{7, 8, 9\}$, 5 seeds), grok-aligning each trajectory to its own accuracy jump, the fraction of units doing genuine two-operand logic goes from 0.006 *before* the grok step to 0.475 *at* it—a step change in logical content locked to the moment the network acquires the capability (Figure 2, left). The contrast with the language-model erosion (right) is the result: same architecture, same measurement, opposite trajectories. The network keeps exactly the logic its objective pays for—crystallizing it at the instant of reasoning, relaxing it away where only prediction is rewarded. "How much logic" is thus not a fixed attribute of the layer but a legible readout of what the task demands of it.

8 Results IV: A Trainability Ceiling at High Boolean Fraction

The architecture of Section 5 is a partition: a fraction of each FFN is the GELU baseline and the remainder is the Boolean block, with the paper's configuration using a 25% Boolean share. A natural question for an *end-to-end*-legible model is how far that share can be pushed— ideally to 100%, a purely Boolean FFN with no GELU at all. We find a sharp obstacle that is not about accuracy but about *optimization*: as the Boolean fraction rises, the model trains normally for a long time and then diverges abruptly, and the more Boolean the FFN, the sooner it does so.

Table 8: Trainability versus Boolean fraction (12L, one epoch, all layers $\{\cap, \setminus\}$, parameter-matched). Below 50% the model completes the epoch; above it, every run diverges, and the divergence step falls as the fraction rises. Single seed per configuration; the 90%/95% ordering is within run-to-run noise.

Boolean fraction	outcome	divergence step
25% (this paper)	completes	—
50%	completes	—
75%	diverges	∼136k
90%	diverges	∼24k
95%	diverges	∼32k
100% (pure)	diverges	∼16k

8.1 The trainable horizon shrinks as the Boolean fraction grows

We trained the 12-layer, 125M-parameter model for one epoch on OpenWebText while sweeping the Boolean fraction (all layers, $\{\cap, \setminus\}$ operators, parameter-matched throughout), and recorded whether each run completed the epoch or diverged. We declare divergence when the *instantaneous* perplexity exceeds 100 after a 15k-step grace window, at which point training is halted automatically and a restartable checkpoint is saved. Table 8 reports the outcome.

The picture is a *trainable-horizon* effect rather than a clean threshold: a 25% or 50% Boolean model trains to convergence (the 50% model reaching a dev perplexity of 21.6 versus the GELU baseline's 19.0), whereas every model above 50% eventually diverges, and the step at which it does so grows shorter as the Boolean share grows—from ∼136k steps at 75% down to roughly sixteen thousand for the pure model. Crucially, the instability is also *latent*: the 75% model trained healthily to step 123k (perplexity ≈ 38, indistinguishable from a stable run) before diverging at 136k, so a run that "looks fine" early is not yet safe. Even a single Boolean-bearing layer in an otherwise-GELU stack is enough to seed the failure, though it postpones it dramatically (a model with the Boolean block in layer 0 only diverged at step 202k).

8.2 The failure is a sudden spike, invisible to the running average

The divergence is not a gradual drift but a near-instantaneous event. Across the 75% model's blow-up, the *cumulative* epoch perplexity moved only from 92 to 94 while the *instantaneous* perplexity jumped from 51 to 305 within a single 250-step logging window. The running average—the quantity ordinarily monitored during training—barely registers the event until it is far advanced, which is why our divergence criterion and the early-stopping guard both operate on instantaneous, not cumulative, loss. We note this as a small methodological point: characterizing this failure mode at all requires watching the instantaneous signal.

8.3 It is not the magnitude of the residual write

A natural hypothesis is that the Boolean block's contribution to the residual stream grows without bound and a single large write destabilizes the model. The Boolean *features* are already bounded—they are sigmoid products in $[0, 1]$—so the only unbounded quantity is the read-out matrix W_o. We tested two interventions that bound the residual write directly. A parallel linear bypass added to a pure Boolean layer delayed its divergence by roughly four-fold (step 16.5k to 69k) but did not prevent it; normalizing the FFN output to unit RMS (a fixed-magnitude residual write regardless of $\|W_o\|$) likewise only postponed the pure model's divergence (to step 19k). *Neither bounding the write nor a stabilizing linear path removes the instability*, which argues against a write-magnitude explanation and points instead to an ill-conditioning of the optimization itself.

A plausible—but unverified—mechanism is consistent with the interpretability measurements of Section 7. Training drives the operand projections well above their initialization scale (the row norm of W_a grows two- to four-fold over training) and pushes roughly half of the operand values into the saturated tails of the sigmoid. In that regime the gradient of a bounded product $\sigma(W_a x)\,\sigma(W_b x)$ is dominated by the small, sharply varying derivative of a saturated sigmoid, and a stack of such layers is prone to the kind of sudden, self-reinforcing

update we observe. A sufficient minority of GELU units—the partition—supplies an unsaturating gradient path that keeps the optimization well-conditioned, which is why a partition buys *horizon* (more Boolean delays the onset) without buying *immunity*.

8.4 Implication

Legibility, in this architecture, is therefore free only up to a partition. At the 25% Boolean share we study, the model trains exactly as well as its GELU baseline; one can push to 50% at a small perplexity cost; but a fully Boolean, end-to-end-legible FFN is not trainable by the present recipe, and the two obvious fixes—bounding the write, adding a linear highway—only delay the failure. The obstacle to an explanatory language model in which *every* feed-forward unit carries explicit logical form is thus not representational but optimization-theoretic: the high-Boolean-fraction ceiling is consistent with a saturated-product gradient that bounding the residual write does not cure. Removing it is the central open problem this work leaves behind.

9 Results V: Self-Forgetting Quantifiers and Legible Licensing

Two results above bound NC-FFN's legibility, and they point the same way. Section 7 found that genuine two-operand logic is realized only at the embedding-adjacent layer and *erodes* toward soft gating under language-model training. Section 6 traced the model's one robust grammatical deficit to a specific cluster of constructions—NPI licensing, long-distance extraction, and quantifiers—i.e. exactly the phenomena a set-logic FFN ought to be good at. Both diagnoses share a cause: the operators of NC-FFN are *within-token*. Intersection and set-difference combine features at the current position; they say nothing about whether a feature has *already occurred* earlier in the sequence, which is what licensing and quantification require ("there is a comparative *somewhere to the left*, so license *than*").

We close the paper by adding the missing primitive—a fuzzy *quantifier* over the sequence—and find that it converts the limitation into the work's strongest legibility result. A small block of *self-forgetting* fuzzy quantifiers (i) recovers the grammatical deficit and modestly exceeds the baseline, (ii) *holds* its logical structure through training—and pushes it *into depth* rather than eroding—and (iii) reads, at the semantic layers, as a bank of grammatical *licensing detectors*: crisp, short-lived, and individually nameable without dictionary learning. The decay is the crux: it is what keeps the quantifier a *predictive, local* operator rather than a sticky latch, and what makes the mechanism fit how a transformer actually processes a sequence.

9.1 A fuzzy-quantifier block with learned forgetting

To the hybrid layer of Section 3.4 (the $\rho = 0.75$ GELU/Boolean partition) we add a third, parameter-neutral block of m_q *quantifier* units. Each unit forms a per-token fuzzy membership from the residual stream,

$$M_t = \sigma(W_q\, x_t) \in [0,1]^{m_q}, \qquad W_q \in \mathbb{R}^{m_q \times d}, \tag{8}$$

and the membership is aggregated *along the sequence* by two causal fuzzy quantifiers, a soft existential and a soft proportion, each with its own *learned* forgetting rate:

$$(\text{"}\exists \text{ recently"}) \quad E_t = \max\big(M_t,\ \gamma \odot E_{t-1}\big), \tag{9}$$

$$(\text{"proportion recently"}) \quad P_t = (1-\lambda) \odot M_t + \lambda \odot P_{t-1}, \tag{10}$$

with per-unit decays $\gamma = \sigma(\theta_\gamma)$ and $\lambda = \sigma(\theta_\lambda)$ in $(0,1)$. The two limits are the non-forgetting quantifiers: $\gamma = 1$ makes (9) a cumulative maximum ("M fired at *some* earlier token"), and $\lambda = 1$ makes (10) a cumulative mean ("the *fraction* of earlier tokens that fired"). We *initialize* the decays near this non-forgetting limit ($\gamma_0, \lambda_0 \approx 0.99$), so the block begins as a true sticky quantifier and must *learn* any forgetting it adopts. The aggregated streams E_t, P_t are written to the residual through the same shared, *zero-initialized* read-out W_o as the Boolean block, so the layer again begins as a pure GELU FFN and wires the quantifiers in only if useful. We study three members of a ladder, each over the same $\{\cap, \setminus\}$ Boolean base: +QUANT (fixed $\gamma = \lambda = 1$, no forgetting), +DECAY (the learned γ, λ above), and +DECAY+GATE (additionally a per-layer scalar gate

Table 9: Adding a sequence quantifier to NC-FFN closes its grammatical deficit and leads the ladder on LAMBADA (12L, parameter-matched, single seed, both epochs). At epoch 1 +DECAY+GATE erases NC-FFN's −0.019 BLiMP deficit (0.810, level with the 0.807 baseline) and posts the best LAMBADA; at epoch 2 the baseline's grammar pulls ahead (0.823) but the quantifier *halves* the now-wider NC-FFN deficit, and +DECAY posts the best LAMBADA of any model here (0.279). The BLiMP recovery is monotone in the decay ladder (+quant < +decay < +decay+gate).

	Epoch 1			Epoch 2		
Model (12L, param-matched)	LAM acc. ↑	LAM ppl. ↓	BLiMP ↑	LAM acc. ↑	LAM ppl. ↓	BLiMP ↑
GELU baseline	0.254	109.4	0.807	0.275	**78.1**	**0.823**
NC-FFN ($\{\cap, \setminus\}$)	0.262	102.4	0.788	0.273	85.5	0.790
+quant (no forgetting)	0.254	110.9	0.795	0.271	94.0	0.793
+decay (learned γ, λ)	0.250	110.3	0.800	**0.279**	87.6	0.800
+decay+gate	**0.271**	**94.6**	**0.810**	0.264	96.3	0.810

$\beta = \sigma(\theta_\beta)$ on the quantifier write, a learned per-depth volume control). Decay and gate parameters are per-unit/per-layer scalars and are parameter-negligible; m_q is chosen to hold the layer parameter-neutral with the 125M baseline. Logically, each unit is a *unary* predicate M quantified over position by (9)–(10): the block adds *monadic* sequence quantification, not n-ary relations, and the licensor-to-licensee dependency it captures is a relation between *positions* bound by the learned decay rather than an n-ary predicate (we return to this scope in Section 10).

9.2 The quantifier recovers the grammatical deficit—and ties LAMBADA on top

The motivating symptom was grammatical: NC-FFN lost −0.019 BLiMP to the baseline, concentrated in licensing (Section 6). Adding the quantifier block *closes that gap at epoch 1* (Table 9). +DECAY+GATE recovers BLiMP to 0.810—level with the 0.807 GELU baseline and well above NC-FFN's 0.788—while simultaneously posting the strongest LAMBADA of any model here (0.271 vs. the baseline's 0.254), at unchanged parameters and on standard attention. The recovery is *monotone in the ladder*: the non-forgetting +QUANT only *partially* closes the gap (0.795, above NC-FFN's 0.788 but short of baseline), +DECAY reaches 0.800, and +DECAY+GATE 0.810—so it is the forgetting, not the bare aggregation, that closes the grammar. Epoch 2 sharpens this: the baseline's grammar pulls ahead (0.823), but the quantifier *halves* NC-FFN's now-wider deficit (0.810 vs. NC-FFN's 0.790), and +DECAY posts the best LAMBADA of any model here (0.279, edging the 0.275 baseline—single seed, so we read it as a tie-or-slight-lead). The mechanism we add to *recover* the licensing deficit is the same one that, below, reads as licensing detectors, and it is the *decay* that makes the quantifier both grammatical and legible.

We read this conservatively—single seed, though now consistent across both epochs—but the qualitative pattern is clean and is corroborated mechanistically below: the FFN block whose *job* is sequence quantification removes the deficit on the grammar that needs sequence quantification. Confirming that the recovery is concentrated in the same licensing subtasks NC-FFN lost (rather than diffuse) is the natural follow-up; here we establish the aggregate recovery and the mechanism behind it.

9.3 Now the structure holds—and migrates into depth

The most worrying property of NC-FFN was dynamic: its two-operand logic was an *early*-training feature that eroded toward soft gating (Section 7.6). The quantifier model does not erode. Re-running the realization probe across the same training checkpoints (50k → 250k → epoch) tells the opposite story (Table 10). The load-bearing intersection signal $\overline{A \cdot B}$ does not collapse to layer 0 and decay; it *redistributes toward depth*—falling at layer 0 (0.059 → 0.037) while the deep layers roughly *double* (L8 0.008 → 0.014, L9 0.011 → 0.018), with the layer-average tracing a shallow U (a mid-training dip that recovers to its starting value by the epoch). Two surface statistics do soften over training (std(B) 0.26 → 0.20, crisp(A, B) 0.53 → 0.48), but the operative quantity—realized two-operand intersection—is held and *deepened*. This is the reversal we were

Figure 3: $A{\cdot}B$ intersection magnitude per layer across epoch-1 training (+DECAY+GATE). Unlike NC-FFN's L0 erosion, the intersection signal migrates out of layer 0 into the deep layers rather than collapsing—genuine two-operand logic is held and pushed into depth.

Table 10: Realization migrates into depth (+DECAY+GATE, $\overline{A \cdot B}$ by layer over training). Contrast Section 7, where NC-FFN's two-operand signal was an L0-only feature that decayed: here it falls at L0 and *rises* in the deep layers.

$\overline{A \cdot B}$	L0	L8	L9	layer-avg
step 50k	0.059	0.008	0.011	U-shape
epoch end	0.037	0.014	0.018	(dips ∼150k, recovers)

after: where the within-token Boolean logic of NC-FFN degenerated to an L0 relic, the sequence-quantifier model spreads genuine logic across the stack and keeps it there (Figure 3).

The decay/gate split also separates here, and it is informative. *Learned decay* preserves quantifier crispness best (shallow layers even sharpen; only the top two or three soften, mean 0.858 → 0.832). The *gate* (+DECAY+GATE) trades some of that away at the deepest layers (0.840 → 0.755; L11 0.83 → 0.51) in exchange for its LAMBADA/BLiMP gains. We accordingly treat +DECAY as the clean mechanistic object and the gate as a performance-oriented depth-shaping refinement.

9.4 The decay un-learns the latch: forgetting, not memory

The quantifiers (9)–(10) *start* as sticky operators ($\gamma_0 \approx 0.99$: a cumulative max never forgets). A model that simply rode that initialization would be implementing a permanent latch—"once true, true forever"—which is not how a language model processes a sequence and would make the operator a poor fit. It does not. Reading the learned decays off the trained weights and converting them to token half-lives $t_{1/2} = \ln(0.5)/\ln\gamma$ shows that *every* unit moved decisively away from the latch (Table 11):

- **No near-permanent units.** Not one of the 1536 existential units (and none of the proportional units) has $\gamma > 0.97$ in either learned model; the maximum is $\gamma = 0.963$, and only 0.07% exceed $\gamma = 0.90$. From a $\gamma_0 \approx 0.99$ start, the decays were *learned down*.
- **Short, local memory.** The median existential half-life is 1.52 tokens (proportional 1.32); 88.5% of existential units forget within two tokens. The quantifier became a short recency detector, not a store.
- **A mid-stack lifetime hump.** Half-life peaks at the middle layers (L4–7, ∼1.7 tokens) and is shortest at the edges (L0, L8–11, ∼1.2–1.4); the per-layer gate β is *highest* exactly where lifetimes are shortest (peak $\beta = 0.80$ at L9), i.e. the model leans on the quantifier most for ephemeral, per-token detection.

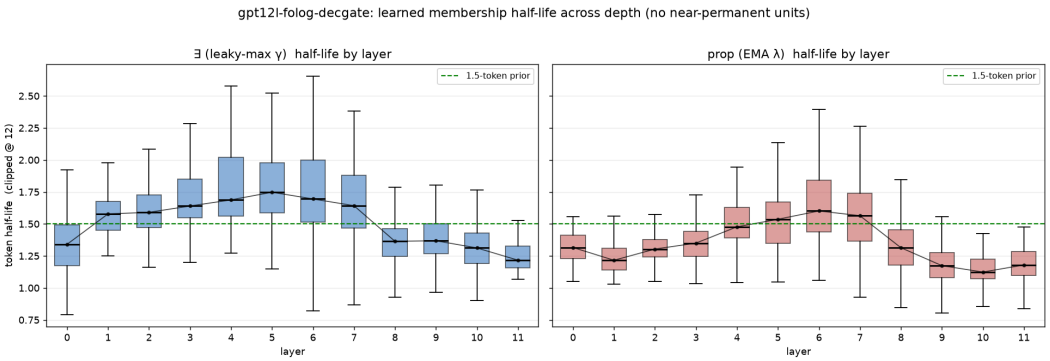

Figure 4: Learned existential (∃) token half-life per layer (median ∼1.5 tokens). From a sticky $\gamma_0 \approx 0.99$ initialization, every unit learned a short, local memory; *zero* units remain near-permanent.

Table 11: Learned forgetting (existential quantifier, both learned models). Initialized at a sticky $\gamma_0 \approx 0.99$ (cumulative max), every unit learned a short half-life; *zero* units remain near-permanent. Half-lives in tokens, $t_{1/2} = \ln(0.5)/\ln\gamma$.

	median $t_{1/2}$	% units < 2 tok	max γ	% units $\gamma > 0.97$
existential (E)	1.52 tok	88.5%	0.963	**0.0%**
proportion (P)	1.32 tok	96.4%	0.955	**0.0%**

That the operator un-learns its own stickiness is the result that makes it transformer-appropriate, and it sets up the reading of the next subsection: a ∼1.5-token memory is precisely long enough to carry a *prediction* from one token to the next, and no longer (Figure 4).

9.5 The legible units are grammatical *licensing detectors*

At the semantic layers where the quantifier write is largest (L9–L11, gate $\beta = 0.80/0.75/0.56$), the membership units are individually nameable, and they realize a single, consistent computation: *predictive grammatical licensing*. Crucially—and this is the cleanest part of the story—a unit does *not* fire on the token it decodes to. Reading a unit's write direction through the unembedding (a logit lens over its W_o column) names a *function word*; but the membership $M = \sigma(W_q x)$ itself fires one token *earlier*, on the grammatical *licensor* that predicts that function word, and the short-memory existential then carries it forward to the position where the function word is emitted. We verified the literal-token reading is false: for the comparative unit, mean membership on ' than' is 0.05, but on its licensors ' more'/' less' it is 0.55–0.64. Four such detectors recur across both learned models (Table 12):

The mechanism is internally coherent in a way that is worth stating, because it explains why the decay was necessary. In the four hand-inspected examples the licensor-to-function-word distance is one or two tokens ("rather than" +1; "turning them into" +2; "neither quick nor" +2), and the learned existential half-life is ∼1.5 tokens. *The decay tuned itself to the grammatical-licensing window*: long enough to carry the membership from the licensor to the licensed position, short enough not to latch and pollute later predictions. The three measurements of this section—recovers the licensing deficit (§9.2), holds and deepens its structure (§9.3), and forgets on a ∼1.5-token timescale (§9.4)—thus compose into one legible operator: *fire on the licensor, decay for ∼one token, write the licensed word* (Figure 5). Each detector is, in effect, a learned, readable fragment of a transformer's grammatical competence—of the kind the BLiMP suite tests directly.

9.6 An honest ceiling: legibility is localized, not network-wide

We resist over-reading the result. Quantifying *how much of the whole network* is human-nameable— combining, per layer, the token-explainability of the FFN units (Boolean and membership, value-vector to

Table 12: Four grammatical *licensing detectors* (layer 9, recurring across the +DECAY and +DECAY+GATE models). The membership fires on the *licensor*; the unit writes toward the *licensed* function word it predicts; the ∼1.5-token decay bridges the gap. None fires on the function word it names.

Construction	fires on (licensor)	writes / predicts	example (M at licensor)
comparison	comparatives (‘ more’, ‘ rather’, ‘ -er’)	‘ than’	“rather” → than (0.95)
passive/agentive	passive participles (‘ made’, ‘ caused’)	‘ by’	“made” → by (0.72)
directional	motion/transformation verbs (‘ turning’, ‘ put’)	‘ into’	“turning” → into (0.84)
disjunction	neg-polarity / alternatives (‘ neither’, ‘ either’)	‘ or’/‘ nor’	“neither” → nor (0.57)

vocabulary against a matched-random floor) with the discernibility of the attention heads (this model uses standard attention; we score each head as crisp-and-nameable or not)—puts the figure at ≈2% of all parameters, or ≈4% if one excludes the deliberate GELU gradient-highway that carries no legibility claim. This is a logit-lens/single-relation concentration proxy, not a causal autointerp score, and it should be read as a floor, not a verdict. The honest summary is that legibility is *localized*: FFN nameability is monotonically back-loaded, near the floor through L1–L7 and rising sharply to L11 (25.6%; membership alone 62.5%), exactly where the licensing detectors live; attention nameability is the mirror image, present only as shallow positional heads (L2–L4, L7) with the deep half opaque. So the claim of this section is precise and bounded: not an understandable network, but a *localized, interpretable-by-construction grammatical mechanism*—a bank of self-forgetting quantifier units that, at the semantic layers, compute readable licensing—living inside an otherwise ordinary transformer, at no parameter cost and no loss of language-model quality. That is still a sharp advance over a standard FFN, whose interpretable-by-construction content is zero.

10 Discussion

What the results say together. The thread connecting capability, language modeling, and legibility is a single claim: a more *structured* FFN reasons more compactly and exposes *how* it computes, at a modest and well-localized cost. Capability makes the “compactly” concrete—a single bounded-multiplicative layer is a more parameter-efficient parity basis than strictly larger GELU (Section 5). Language modeling shows the cost is real but small and, tellingly, that the capability is *dormant* for next-token prediction, which does not reward products (Section 6). Legibility delivers the “how”—explicit per-unit logical form, a directly readable subset, causally-used features—and the dynamics tie it back to capability: the logic *is* the reasoning, crystallizing when the task rewards it and relaxing when it does not (Section 7.6).

The sequence operator turns the limitations into the headline. Two of those findings are limitations, and they share a cause: the set operators are *within-token*, so they cannot express that a feature occurred earlier in the sequence (Section 9). Supplying the missing primitive—a fuzzy quantifier over the sequence with a *learned* forgetting rate—is the paper’s strongest result, and it is striking for three reasons. First, the mechanism we add to *recover* the licensing deficit is the same one that, read out, *is* the licensing: the block whose job is sequence quantification both closes the grammar gap and exposes a bank of grammatical licensing detectors. Second, the legibility no longer erodes—it holds and migrates into depth—so the dynamic relaxation we documented for the within-token operators is specific to them, not to structured FFNs in general. Third, and most telling for whether the operator belongs in a transformer at all, the decay *un-learns* its own stickiness: from a sticky cumulative-max initialization every unit learns a short, ∼1.5-token half-life, and that half-life turns out to match the one-to-two-token distance from a grammatical licensor to the word it licenses. The model was free to keep a permanent latch and instead learned a local, predictive operator—exactly the temporal logic a left-to-right language model can use—and the licensing detectors are what that operator looks like when it is read.

What kind of logic this is—and what it is not. It is worth stating the scope of the “logic” precisely, because the architecture invites a natural misreading. The set operators are *unary* predicates of a single

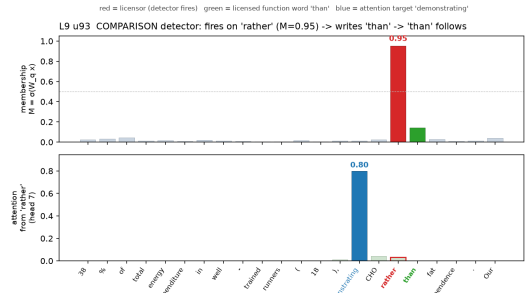

(a) Comparison detector: fires on comparatives (‘rather’/‘more’) and predicts ‘than’.

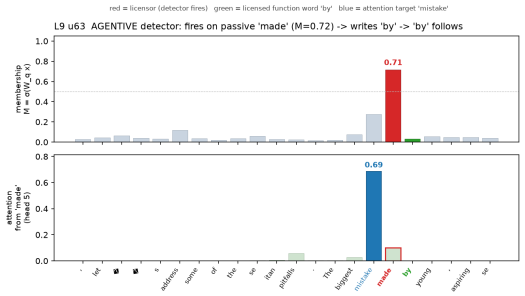

(b) Agentive detector: fires on passive participles (‘made’/‘caused’) and predicts ‘by’.

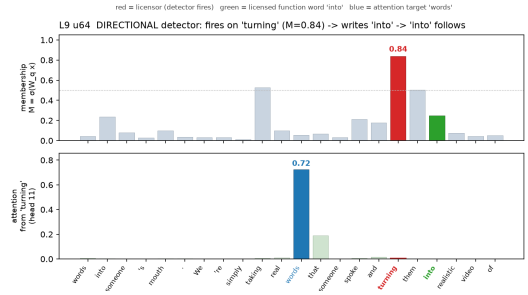

(c) Directional detector: fires on motion verbs (‘turning’/‘put’) and predicts ‘into’.

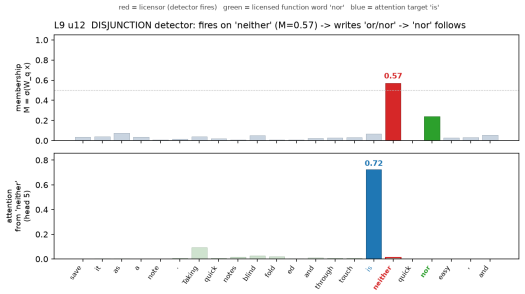

(d) Disjunction detector: fires on ‘neither’/‘either’ and predicts ‘or’/‘nor’.

Figure 5: Four grammatical *licensing detectors* (layer 9), each a predictive operator. Membership fires crisply on the grammatical *licensor* (left spike), the ∼1.5-token existential decay carries the signal forward over the licensing window, and the unit writes the *licensed* function word it predicts. None fires on the function word it names.

token’s representation, and intersection and set-difference are *propositional* connectives over them; the quantifiers (9)–(10) range over the *positions* of a unary predicate. The fragment is therefore *monadic* predicate logic—unary predicates with quantification over the single sequence variable—*not* n-ary relational logic, and we make no claim to relational expressiveness. This is a scope, not a shortfall, for two reasons. First, monadic-with-sequence-quantification is already strictly stronger than propositional: an existential over the prefix *binds a variable*—“a feature occurred at some earlier position”—which no within-token propositional layer can express, and it is exactly the fragment a left-to-right model needs for the licensing dependencies we study. Second, the dependency the quantifier captures—a licensor at one position to the word it licenses at another—is a relation between *positions*, bound by the decay-quantifier, not a relation between argument slots at one token: the “second argument” is the other position, and the learned decay is what binds it. NC-FFN’s operators are *asymmetric* by construction ($A \setminus B \neq B \setminus A$; existential $\neq$ proportion), which is also why a unit’s two operands do not degenerate into a redundant representation: measured directly, redundant operand pairs are under 5% of units, the rest either keeping independent operands or cleanly retiring one to a single operand (Table 5). We therefore keep the FFN’s legible logic monadic and leave relational binding to attention; the contribution is the legibility and the discovered licensing structure, not expressiveness beyond the monadic fragment. Explicit n-ary relational binding—role–filler structure rather than a single quantified variable—is a different mechanism again, the province of tensor-product representations (Smolensky, 1990) and the relational reading of tensor logic (Domingos, 2025); how to incorporate such constructions effectively we leave to future work.

Multiplicativity, bounding, negation: a decomposition of the design. The capability probe lets us assign roles to the properties NC-FFN adds over a GELU FFN. *Multiplicativity* is what does parity at all. *Bounding* is what makes a multiplicative basis usable in width (and so shallow), at the price of depth-

composition—a genuine trade, not a strict improvement, since unbounded products are the better deep basis. *Negation* (the explicit complement) adds a small shallow capability margin but is primarily a *legibility* feature: it turns the layer's products into named set operations and is what makes the readable units read as AND/AND-NOT predicates. We are deliberate that the headline capability is a property of the bounded multiplicative basis, shared with sigmoid-bilinear; the negation's distinctive contribution is interpretive.

Limitations. The language-model results are single-seed at one scale (125M); the BLiMP deficit and the perplexity tie are robust, but the finer downstream numbers want replication. The capability probe is a single synthetic family (parity) under a fixed optimization budget; it measures a real property—per-parameter reasoning efficiency—but a longer budget would let unbounded products' degree-2^L advantage carry further at depth, and other reasoning families may apportion the width/depth axes differently. And the directly-legible units are a small minority; the bulk of operands are distributed, so NC-FFN buys an explicit combination *rule* for free but not, in general, monosemantic operands. The quantifier results (Section 9) are likewise single-seed, though now reported across both epochs; the aggregate grammatical recovery, the learned-forgetting statistics, and the licensing detectors are clear, but a seed sweep and a per-subtask attribution of the BLiMP recovery remain to be run. And the whole-network legibility figure we report is a logit-lens concentration proxy, not causal autointerp, and it is localized to a few late layers—a readable mechanism inside the network, not a readable network.

A trainability boundary, and a path to a fully-legible LM. The stabilizing GELU partition is required, not merely convenient. Section 8 characterizes a *Boolean-fraction-dependent* trainability horizon: at or below an even split the model trains a full epoch, but above it every run descends normally and then diverges abruptly—and the more Boolean the layer, the sooner, from ∼136k steps at 75% down to ∼16k for a fully Boolean FFN. Tellingly, the two obvious remedies—normalizing the residual write to unit magnitude, and adding a parallel linear highway—each only *delay* the divergence rather than prevent it, which points the cause at a saturated-product gradient pathology (the interaction of sigmoid saturation, composition, and the residual stream) rather than the magnitude of the write. This is the chief obstacle to an *end-to-end*-legible language model, in which every FFN unit—not three-quarters of the budget—is a named set operation. Having characterized the instability, we regard *removing* it—most plausibly through a remedy aimed at the saturated-product gradient rather than the residual write—as the most promising next step: it is the difference between a legible *component* and a legible *model*.

Where the capability should pay off. Because the capability is dormant for next-token prediction, the natural place to look for a *performance* win is tasks that reward multiplicative composition—symbolic, arithmetic, and algorithmic reasoning—rather than open-web language modeling. The width/depth dissociation also suggests a concrete design lever: bounded blocks where shallow, width-cheap logic is wanted; unbounded (or hybrid) blocks where deep compositional reach is. We leave both to future work.

11 Conclusion

We studied a parameter-neutral transformer FFN whose hidden units are explicit fuzzy set operations, with a bounded complement that gives negation a clean positive form. The choice is not free—it costs a little grammar and needs a stabilizing partition—but it buys two things an opaque activation does not. It reasons more compactly: on a controlled probe, bounded multiplicative units are the most parameter-efficient reasoning basis at shallow depth, and the properties we toggle (multiplicativity, bounding) cleanly govern the width and depth axes of that efficiency. And it is legible: every unit is a named operation, a subset reads as predicates, and the network's logical content is a dynamic readout of what its objective rewards, crystallizing at the moment of reasoning and eroding where only prediction is. And when those within-token operators are given an explicit *sequence* companion—a fuzzy quantifier free to learn how long to remember—the FFN's hardest grammatical failures become its most legible mechanism: a bank of *self-forgetting* quantifier units that, at the semantic layers, compute readable grammatical *licensing*, recover the grammar deficit at no parameter or quality cost, and each learn a memory just long enough to carry a licensor to the word it licenses. That legibility is for now free only up to a partition: a stabilizing GELU fraction is required, and

training a fully Boolean, end-to-end-legible model—removing the trainability boundary of Section 8—is the open problem we leave. A structured component, in short, lets us ask not just what a feed-forward layer represents but how it combines—and, with an explicit sequence operator, how it *licenses*—and, increasingly, get an answer.

References

Samy Badreddine, Artur d'Avila Garcez, Luciano Serafini, and Michael Spranger. Logic tensor networks. *Artificial Intelligence*, 303, 2022.

Trenton Bricken, Adly Templeton, Joshua Batson, Brian Chen, Adam Jermyn, et al. Towards monosemanticity: Decomposing language models with dictionary learning. *Transformer Circuits Thread*, 2023.

Xuelu Chen, Ziniu Hu, and Yizhou Sun. Fuzzy logic based logical query answering on knowledge graphs. In *AAAI Conference on Artificial Intelligence*, 2022.

Peter Clark, Isaac Cowhey, Oren Etzioni, Tushar Khot, Ashish Sabharwal, Carissa Schoenick, and Oyvind Tafjord. Think you have solved question answering? try ARC, the AI2 reasoning challenge. *arXiv preprint arXiv:1803.05457*, 2018.

Hoagy Cunningham, Aidan Ewart, Logan Riggs, Robert Huben, and Lee Sharkey. Sparse autoencoders find highly interpretable features in language models. In *International Conference on Learning Representations (ICLR)*, 2024.

Yann N. Dauphin, Angela Fan, Michael Auli, and David Grangier. Language modeling with gated convolutional networks. *International Conference on Machine Learning (ICML)*, 2017.

Pedro Domingos. Tensor logic: The language of AI. *arXiv preprint arXiv:2510.12269*, 2025.

Nelson Elhage, Tristan Hume, Catherine Olsson, Neel Nanda, Tom Henighan, et al. Softmax linear units. *Transformer Circuits Thread*, 2022a.

Nelson Elhage, Tristan Hume, Catherine Olsson, Nicholas Schiefer, Tom Henighan, et al. Toy models of superposition. *Transformer Circuits Thread*, 2022b.

Leo Gao, Jonathan Tow, Stella Biderman, Sid Black, et al. A framework for few-shot language model evaluation. EleutherAI lm-evaluation-harness, Zenodo, https://doi.org/10.5281/zenodo.5371628, 2021.

Felix A. Gers, Jürgen Schmidhuber, and Fred Cummins. Learning to forget: Continual prediction with LSTM. *Neural Computation*, 12(10):2451–2471, 2000.

Mor Geva, Roei Schuster, Jonathan Berant, and Omer Levy. Transformer feed-forward layers are key-value memories. In *Empirical Methods in Natural Language Processing (EMNLP)*, 2021.

Yongchao Huang and Hassan Raza. Semantic fusion with fuzzy-membership features for controllable language modelling. *arXiv preprint arXiv:2509.13357*, 2025.

Denis Paperno, Germán Kruszewski, Angeliki Lazaridou, Quan Ngoc Pham, Raffaella Bernardi, Sandro Pezzelle, Marco Baroni, Gemma Boleda, and Raquel Fernández. The LAMBADA dataset: Word prediction requiring a broad discourse context. In *Association for Computational Linguistics (ACL)*, 2016.

Michael T. Pearce, Thomas Dooms, and Alice Rigg. Weight-based decomposition: A case for bilinear MLPs. *arXiv preprint arXiv:2406.03947*, 2024.

Michael T. Pearce, Thomas Dooms, Alice Rigg, Jose Oramas, and Lee Sharkey. Bilinear MLPs enable weight-based mechanistic interpretability. *International Conference on Learning Representations (ICLR)*, 2025. arXiv:2410.08417.

Felix Petersen, Christian Borgelt, Hilde Kuehne, and Oliver Deussen. Deep differentiable logic gate networks. In *Advances in Neural Information Processing Systems (NeurIPS)*, 2022.

Felix Petersen, Hilde Kuehne, Christian Borgelt, Julian Welzel, and Stefano Ermon. Convolutional differentiable logic gate networks. In *Advances in Neural Information Processing Systems (NeurIPS)*, 2024.

Hongyu Ren and Jure Leskovec. Beta embeddings for multi-hop logical reasoning in knowledge graphs. In *Advances in Neural Information Processing Systems (NeurIPS)*, 2020.

Hongyu Ren, Weihua Hu, and Jure Leskovec. Query2box: Reasoning over knowledge graphs in vector space using box embeddings. In *International Conference on Learning Representations (ICLR)*, 2020.

Ryan Riegel, Alexander Gray, Francois Luus, Naweed Khan, Ndivhuwo Makondo, Ismail Yunus Akhalwaya, et al. Logical neural networks. *arXiv preprint arXiv:2006.13155*, 2020.

Keisuke Sakaguchi, Ronan Le Bras, Chandra Bhagavatula, and Yejin Choi. WinoGrande: An adversarial winograd schema challenge at scale. *AAAI Conference on Artificial Intelligence*, 2020.

Noam Shazeer. GLU variants improve transformer. *arXiv preprint arXiv:2002.05202*, 2020.

Paul Smolensky. Tensor product variable binding and the representation of symbolic structures in connectionist systems. *Artificial Intelligence*, 46(1–2):159–216, 1990.

Alex Tamkin, Mohammad Taufeeque, and Noah D. Goodman. Codebook features: Sparse and discrete interpretability for neural networks. *arXiv preprint arXiv:2310.17230*, 2023.

Andrew Trask, Felix Hill, Scott Reed, Jack Rae, Chris Dyer, and Phil Blunsom. Neural arithmetic logic units. *Advances in Neural Information Processing Systems (NeurIPS)*, 2018.

Emile van Krieken, Erman Acar, and Frank van Harmelen. Analyzing differentiable fuzzy logic operators. *Artificial Intelligence*, 302, 2022. arXiv:2002.06100.

Alex Warstadt, Alicia Parrish, Haokun Liu, Anhad Mohananey, Wei Peng, Sheng-Fu Wang, and Samuel R. Bowman. BLiMP: The benchmark of linguistic minimal pairs for english. *Transactions of the Association for Computational Linguistics (TACL)*, 2020.

Rowan Zellers, Ari Holtzman, Yonatan Bisk, Ali Farhadi, and Yejin Choi. HellaSwag: Can a machine really finish your sentence? In *Association for Computational Linguistics (ACL)*, 2019.

Zhanqiu Zhang, Jie Wang, Jiajun Chen, Shuiwang Ji, and Feng Wu. ConE: Cone embeddings for multi-hop reasoning over knowledge graphs. In *Advances in Neural Information Processing Systems (NeurIPS)*, 2021.